chains wind wildly and exhibit a broad range of hydrogen bond geometries. There is certainly no preference for coplanar dimers. The same description applies to liquid NMA except that few monomers participate in more than two hydrogen bonds so there is little branching of the chains. Local order is also evident in liquid DMF, although it is not as easy to characterize. Near neighbors definitely organize to provide favorable Coulombic interactions. Short contacts between oxygen and the methyl groups are particularly common. Some neighbors with roughly anti-parallel dipoles are apparent. However, this is not a striking feature and seems to be hidden by the apparent medium and long-range disorder.

Conclusion

Optimized intermolecular potential functions have been derived for use in fluid simulations of amides and peptides. The functions have been demonstrated to yield reasonable energetic and structural descriptions of amide dimers and amide–water complexes. Moreover, the principal support for their validity comes from results of Monte Carlo simulations of liquid formamide,

NMA, and DMF. The computed heats of vaporization and densities of the liquids are in essentially exact accord with experimental data. Agreement with available diffraction data on peak positions for radial distribution functions is also excellent. In addition, the simulations yielded thorough descriptions of the structure and hydrogen bonding in the liquid amides. The dominance of hydrogen-bonded chains in liquid formamide and NMA was confirmed, while more subtle local order is apparent in DMF as revealed by dipole correlation functions. The simplicity, form, and demonstrated utility of the OPLS functions make them suitable for study of a wide range of organic and biochemical systems.

How Carbon Monoxide Bonds to Metal Surfaces

Shen-Shu Sung and Roald Hoffmann*

Contribution from the Department of Chemistry, Cornell University, Ithaca, New York 14853. Received May 9, 1984

Abstract: An analysis is presented of the similarities and differences in the bonding of CO to Ni(100), Ni(111), Co(0001), Fe(110), Cr(110), and Ti(0001). The primary interactions in every case are the expected forward and back donation, the mixing of CO 5σ with surface d_{z^2} and s states, and the mixing of CO 2π with metal $d_{xz,yz}$. The latter interaction is dominant. Projections of the density of states and crystal orbital overlap population curves show these interactions clearly. As the metal changes from Ni to Ti, the effects of the rise of the Fermi level and the diffuseness of the d orbitals combine to put more and more electron density into 2π of CO. This is why CO dissociates on the earlier transition-metal surfaces. Our studies of surface coverage show little effect on the diatomic dissociation. There is some indication in the calculations that higher index surfaces should dissociate CO more readily than the lower index ones, but the effect is smaller than that of changing the metal.

The chemisorption of CO on transition-metal surfaces has been the subject of numerous experimental and theoretical studies over the past few decades.[1-6] Brodén, Rhodin, et al. have succeeded in establishing a criterion for dissociative chemisorption behavior of carbon monoxide on a number of transition-metal surfaces as a function of the position of the metal in the periodic table.[1] On the left side of the first-row transition metals, up to Fe, the adsorption is likely to be dissociative. On the right side from Co, it is molecular. Experimental results are available for Ti,[2] Fe,[3] Co,[4] and Ni[1b] in the first row.

In this report we analyze and discuss the electronic consequences of the chemisorption of CO on several transition metals, by using tight binding calculations of the extended Hückel type. Monolayers of CO, CO on Ni(100), comparisons of different metals, different coverages, and different surfaces of the same metal will be studied in this contribution.

Monolayers of CO

The molecular orbitals of an isolated CO molecule are well-known.[7] The highest occupied molecular orbital (HOMO) is mainly a carbon lone pair, as indicated schematically in **1a**.
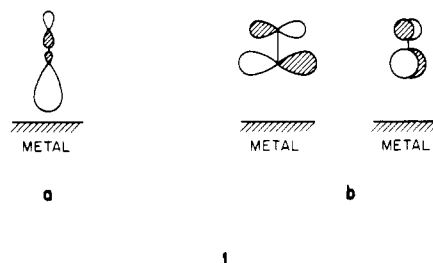
Its energy (ca. −14 eV)[8] is lower than the d states of transition metals. In the generally accepted end-on CO chemisorption configuration the 5σ is pushed down by surface states, relative to other CO levels. The lowest unoccupied molecular orbital set (LUMO) of the free CO molecule, 2π, consists of two antibonding

(1) (a) Brodén, G.; Rhodin, T. N.; Brucker, C.; Benbow, R.; Hurych, Z. *Surf. Sci.* **1976**, *59*, 593. (b) Engel, T.; Ertl, G. *Adv. Catal.* **1979**, *28*, 1.

(2) Eastman, D. E. *Solid State Commun.* **1972**, *10*, 933.

(3) Brodén, G.; Gafner, G.; Bonzel, H. *Appl. Phys.* **1977**, *13*, 33; Jensen, E. S.; Rhodin, T. N. *Phys. Rev. B* **1983**, *27*, 3338.

(4) Greuter, F.; Heskett, D.; Plummer, E. W.; Freund, H. J. *Phys. Rev. B* **1983**, *27*, 7117.

(5) (a) Blyholder, G. *J. Phys. Chem.* **1964**, *68*, 2772. (b) Anderson, A. B. *J. Chem. Phys.* **1976**, *64*, 4046. (c) van Santen, R. A. *Proc. Int. Cong. Catal., 8th* **1984**.

(6) Andreoni, W.; Varma, C. M. *Phys. Rev. B* **1981**, *23*, 437. Allison, J. N.; Goddard, W. A., III *Surf. Sci.* **1981**, *110*, L615. Doyen, G.; Ertl, G. *Surf. Sci.* **1977**, *B5*, 641. Doyen, G.; Ertl, G. *Surf. Sci.* **1977**, *69*, 157. Bagus, P. S.; Hermann, K. *Phys. Rev. B.* **1977**, *16*, 4195. Davenport, J. W. *Phys. Rev. Lett.* **1976**, *36*, 945. Bullett, D. W.; Cohen, M. L. *J. Phys.* **1977**, *C10*, 2101.

(7) (a) Jorgensen, W. L.; Salem, L. "The Organic Chemists Book of Orbitals"; Academic Press: New York 1973; p 78. (b) Huo, W. M. *J. Chem. Phys.* **1964**, *43*, 624. McLean, A. D.; Yoshimine, M. *IBM J. Res. Dev. Suppl.* **1968**, *3*, 206.

(8) Gelius, U.; Basiler, E.; Svensson, S.; Bergmark, T.; Siegbahn, K. *J. Electron Spectrosc. Relat. Phenom.* **1973**, *2*, 405. Turner, D.; Baker, C.; Baker A. D.; Brunkle, C. R. "Molecular Photoelectron Spectroscopy"; Wiley-Interscience: New York, 1970
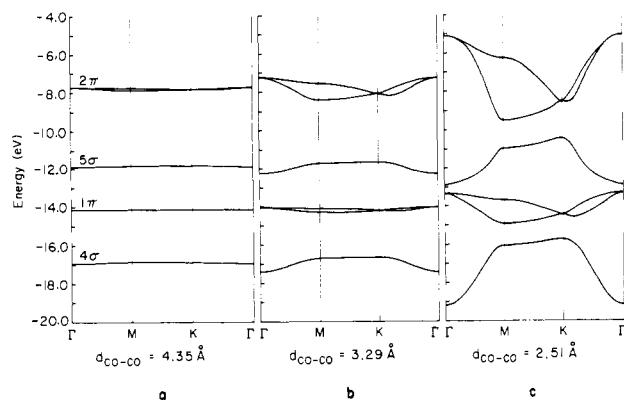
How Carbon Monoxide Bonds to Metal Surfaces

J. Am. Chem. Soc., Vol. 107, No. 3, 1985 579

Figure 1. Band structures of monolayer CO along the symmetry lines indicated by ΓM, MK, and KΓ for CO–CO distances 4.35, 3.29 and 2.51 Å.

orbitals with larger coefficients at the carbon atom, as shown in **1b**. In the absorption the 2π derived orbitals are partially populated and the CO bond weakened. That the 2π orbitals play a crucial role in CO dissociation is a general conclusion previously reached by others, and it will be supported by our calculations. Below these frontier orbitals there are the other 1π, 4σ, 3σ, ... orbitals, which are involved very little in the chemisorption.

Let us first see what the band structure of a CO monolayer looks like. Plummer and co-workers have measured the band structure for CO adsorbed on a Co(0001) surface at $(\sqrt{3}\times\sqrt{3})R30°$ (coverage $\theta = \frac{1}{3}$ monolayer) and $(2\sqrt{3}\times2\sqrt{3})R30°$ ($\theta = \frac{7}{12}$ monolayer) and compared with their tight-binding calculations.[4] These assumed only nearest neighbor interactions with ab initio wave functions or CNDO-type wave functions. Corresponding to the above $\theta = \frac{1}{3}$, $\theta = \frac{7}{12}$ coverages and a hypothetical $\theta = 1$ coverage we carried out tight-binding calculations of the extended Hückel type for hexagonal monolayer CO with nearest neighbor distances of 4.35, 3.29, and 2.51 Å (the nearest neighbor Co and Ni contacts are 2.51 and 2.49 Å, respectively). From the calculated band structure, Figure 1, we see that at the distance of 4.35 Å, Figure 1a, the CO–CO interaction is negligible; at 3.29 Å, Figure 1b, the interaction is turned on; and at 2.51 Å, Figure 1c, the band widths attain several electron volts. Especially the 2π band dispersion is large, over 4 eV. CO–CO interaction has been discussed elsewhere, notably by Plummer and co-workers[4] and by Anderson.[9] In our subsequent computations of CO on metal surfaces we will often choose a high coverage, for reasons of computational economy. The resulting CO band widths will be inherently high, due to CO–CO interactions. They will often be higher than the experimental results, which are usually for lower coverage.

CO Chemisorption on the Ni(100) Surface

We eventually will compare the behavior of CO on various surfaces—Ni(100), Ni(111), Co(0001), Fe(110), Cr(110), and Ti(0001). But let us begin with the best known system the c-(2×2)CO–Ni(100). The geometry of this surface, in two views, parallel and perpendicular to the surface, is shown in **2**.

From top   From side

○ Ni atom

○ C atom

○ O atom

2

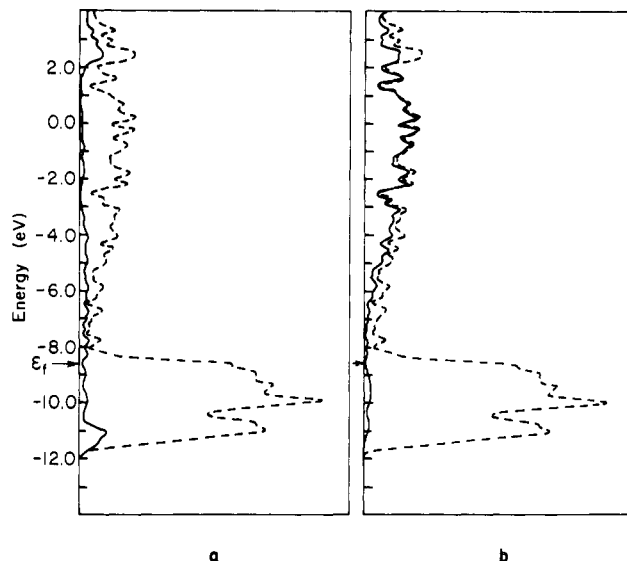(9) Anderson, A. B. *Surf. Sci.* **1977**, *62*, 119.
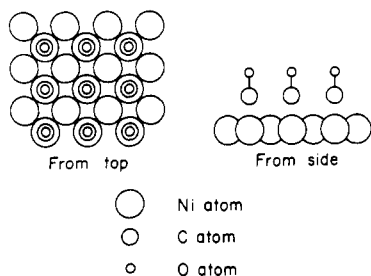
Figure 2. Projected DOS of a Ni(100) four-layer slab. The solid line indicates s states in part a and p states in part b. The broken lines are the total DOS in both parts a and b. The peak between -8 and -12 eV indicates mainly d states penetrated by s and p states.

It is known experimentally that the CO molecule is chemisorbed with its molecular axis normal to the surface and its carbon end closer to the Ni atom.[10,11] The C–O bond length is 1.1 ± 0.1 Å.[11]

In order to achieve the best compromise between time of computation and accuracy of the model, we chose to use a four-layer-slab model of the metal surface. From previous work in our group,[12] reasonable convergence is reached for such a four-layer-slab model. A 15K point set[13] was used for the square lattice. The CO molecules are adsorbed on one side of the slab. When CO molecules are adsorbed on both sides of the metal slab, the calculated electron densities on the inner-layer atoms are different from those when CO molecules are adsorbed on one side. However, the electron densities on CO and on the surface metal atoms bearing CO, which we focus on in this paper, are very similar to those in the case of single-face adsorption. The Ni–C distance is taken as 1.8 Å.[11] Further details of the computations are given in the Appendix.

Without adsorbate the clean Ni(100) slab is characterized by the calculated density of states (DOS) of Figure 2. The d states form a band of ~4 eV width; the s and p bands are much wider. Note the substantial penetration of the d band by the s, p bands. If we look at the detailed composition of, say, the surface layer of the slab, we obtain the orbital populations $d^{9.370}s^{0.618}p^{0.186}$, not very different from the usual assumption of d^9s^1. Note the surface layer is negatively charged. This has been given a simple explanation in a previous paper from our group[12] and in the work of others.[14,15] Simply speaking, the surface states are less dispersed because the surface atoms have fewer nearest neighbors than bulk atoms do. It follows that for d electron counts corresponding to more than half-filling the d band, the surface is more negative than the bulk, while for low-electron counts the surface should be positive. The smaller dispersion of the surface states may be seen in Figure 3, which shows the fraction of the total slab DOS which is on the surface layers and that which is on the inner,

(10) (a) Allyn, C.; Gustafsson, T.; Plummer, E. *Solid State Commun.* **1978**, *28*, 85. (b) Passler, M.; Ignatiev, A.; Jona, F.; Jepsen, D.; Marcus, P. *Phys. Rev. Lett.* **1979**, *43*, 360.

(11) Anderson, S.; Pendry, J. *Phys. Rev. Lett.* **1979**, *43*, 363.

(12) Saillard, J.-Y.; Hoffmann, R. *J. Am. Chem. Soc.* **1984**, *106*, 2006.

(13) Pack, J. D.; Monkhorst, H. J. *Phys. Rev. B* **1977**, *16*, 1748.

(14) (a) Shustorovich, E.; Baetzold, R. C. *J. Am. Chem. Soc.* **1980**, *102*, 5989. (b) Shustorovich, E. *J. Phys. Chem.* **1982**, *86*, 3114. (c) Shustorovich, E. *Solid State Commun.* **1982**, *44*, 567.

(15) Feibelman, P. J.; Hamann, D. R. *Solid State Commun.* **1979**, *31*, 413. Desjonqueres, M. C.; Spanjaard, D.; Lassailly, Y.; Guillot, C. *Solid State Commun.* **1980**, *34*, 807.
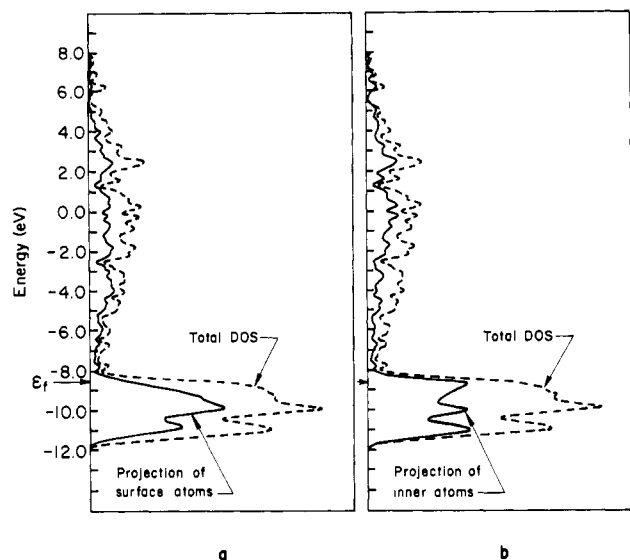
Figure 3. Projected DOS of surface and inner layers of a Ni(100) four-layer slab. In better, self-consistent calculations similar dispersing effects are observed, but the surface states are more skewed toward the Fermi level.
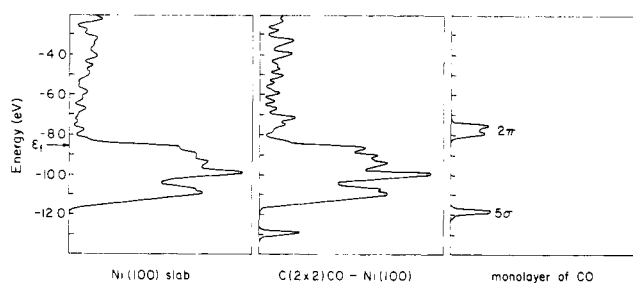

Figure 4. Total DOS of a Ni(100) slab, a c(2×2)CO–Ni(100) system, and a monolayer of CO.

Table I. Calculation Results on c(2×2)CO–Ni(100)

Overlap Populations	
M–C	0.84
C–O	1.04 (1.21 in free CO)
CO Electron Densities	
5σ	1.62 (2 in free CO)
2π	0.37^c (0 in free CO)
Electron Density Changes on Surface Atoms[a]	
Δs	−0.05
Δp_σ	0.17
Δp_π	0.04
Δd_σ	−0.50
Δd_π	−0.50
Δd_δ	0.03
total	−0.80
energy change,[b] ΔE, eV	−2.43

[a] Electron density changes of those surface atoms having adsorbed CO on it. [b] E(Ni slab and adsorbed CO) − E(Ni slab and separated CO) for one unit cell, i.e., eight Ni atoms and one CO. [c] This is the electron density in each of the 2π orbitals, that is, the two degenerate 2π orbitals gain 0.74 e altogether.

bulk-like layers. In better, self-consistent calculations similar dispersion effects are observed, but the surface states are more skewed toward the Fermi level.

Now let us see what happens when the c(2×2)CO–Ni(100) system is assembled. At left in Figure 4 is the DOS of the naked slab, at right the isolated CO layer, and in the center the composite surface plus overlayer. The electron-density changes are best indicated in tabular form (Table I).

The density of states curve clearly shows that the major surface–adsorbate interactions involve the 5σ and 2π orbitals of the carbon monoxide. The surface Ni d electron densities decrease
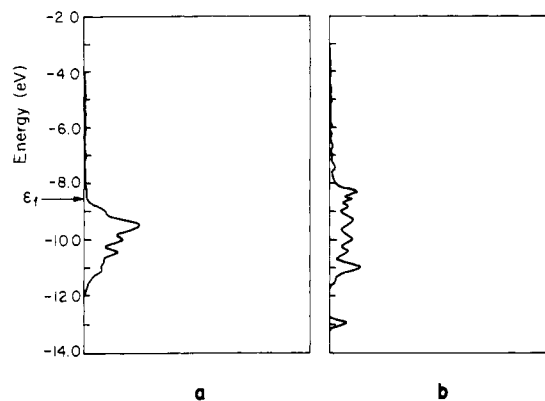

Figure 5. Projected DOS of d_{z^2} of (a) a clean surface layer and (b) those surface atoms having adsorbed CO. The increase of DOS above the Fermi level in part b, compared to that in part a, corresponds to the 0.50 electron density decrease in d_{z^2} (see Table I).
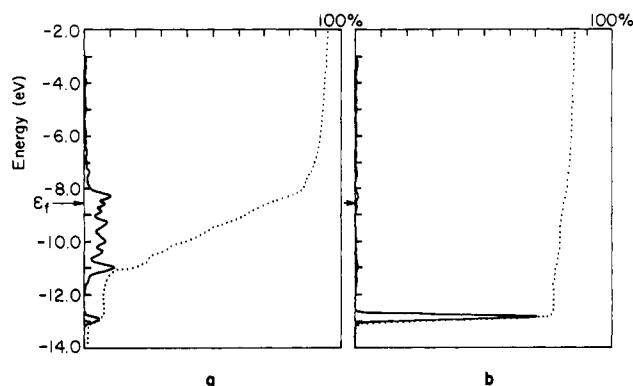

Figure 6. Projected DOS of (a) d_σ of those surface atoms which have CO adsorbed on them and (b) 5σ of CO in the c(2×2)CO–Ni(100) system. The dotted line is an integration. Those states above the Fermi level in part b illustrate the electron density decrease from 2 to 1.62 (see Table I).

dramatically, in both the σ and π components.

The electron density in d_σ, or d_{z^2}, if we take the normal of Ni surface as the Z direction, changes substantially. The d_{z^2} orbitals are pointed directly toward the CO 5σ orbitals, **3**, and are at higher

3

energy than CO 5σ. The interaction pushes the d_{z^2} orbitals up, and consequently a greater portion of the d_{z^2} band rises above the Fermi level. Since the d states are nearly completely filled for the clean surface, this interaction decreases the d_{z^2} electron density. The projected d_{z^2} DOS in the chemisorption system is shown in Figure 5. Comparison with the naked surface clearly shows the shift in density that is described above. We will see later that as one goes from Ni to Ti, the d orbitals are less populated for the surface and the d_σ density changes consequently become smaller.

There is no contradiction between the concept of strong metal–CO 5σ orbital interaction, with consequent d_{z^2} (and to a smaller extent s) depletion, and the generally accepted notion of CO-to-metal electron transfer. The 5σ loses electron density, its population going from 2.0 in the free molecule to 1.62 in the chemisorbed system. The states which are pushed up above the Fermi level, and which we said originated from d_{z^2}, are in reality an antibonding mixture of d_{z^2} and 5σ orbitals, and vacating them
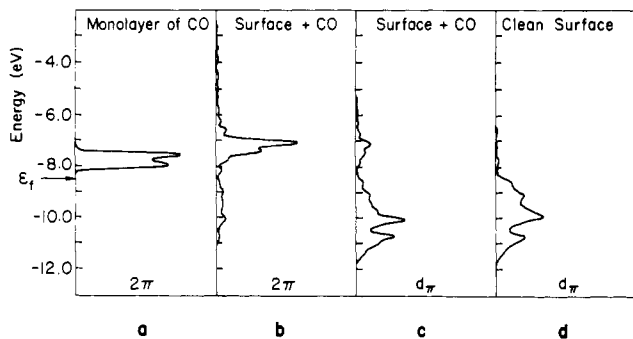
How Carbon Monoxide Bonds to Metal Surfaces

J. Am. Chem. Soc., Vol. 107, No. 3, 1985 581

Figure 7. Projected DOS for (a) 2π of a monolayer of CO, (b) 2π of the same CO, adsorbed, (c) d_π levels of those surface atoms having adsorbed CO, and (d) d_π of the clean metal surface.

depletes both metal d_σ and 5σ of carbonyl. Figure 6 shows how the metal d_σ and carbonyl 5σ electron densities are correlated.

Another significant change in the electron densities of the Ni surface is in the d_π or $d_{xz,yz}$ orbitals. These orbitals are pointed directly toward the CO 2π orbitals (with overlap 0.12 in a fragment) and the 1π orbitals (with overlap 0.04). The 1π orbitals of CO are bonding between C and O, with the larger component on the oxygen atom and major electron density in the region between C and O. Their overlap with d_π is much smaller than that of the 2π set. The energy of the 1π orbitals is several electron volts below the corresponding value of the metal d electrons. Therefore, the 1π orbitals are essentially not involved in metal–CO interaction. The 2π set is quite different. These orbitals are antibonding between C and O with larger components on the carbon atom and an energy very close to transition metal $d_{xz,yz}$, **4**. They interact strongly with metal d_π or $d_{xz,yz}$ orbitals.

4
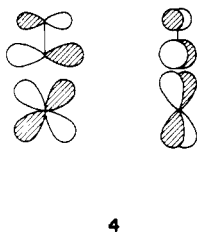
We can follow this π interaction in a number of ways. First we see that 2π is populated by 0.37 and d_π depleted by 0.495 e. This is once again the result of interaction between the two level types shifting some of the d_π density above the Fermi level. The projections of the DOS before and after interaction (Figure 7) clearly show the buildup of density in one orbital in the energy region of the other.

Another way to follow the involvement of the various orbitals in bond formation is through crystal orbital overlap population (COOP) curves.[16] The COOP is really an overlap population weighted density of states, i.e., it weights the DOS in each energy interval by its contribution to the overlap population. In Figure 7 we saw in the d_π and 2π projections a buildup of electron density in two regions, at -10, -11 and around -7 eV. We would suspect that these regions correspond to metal–CO π bonding and antibonding combinations, respectively. Schematic drawings are given in **5** and **6**. Note that whereas **5** and **6** differ in M–CO

5   **6**
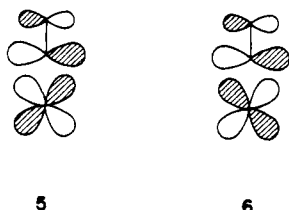
bonding, they are both C–O antibonding. Figure 8 shows the

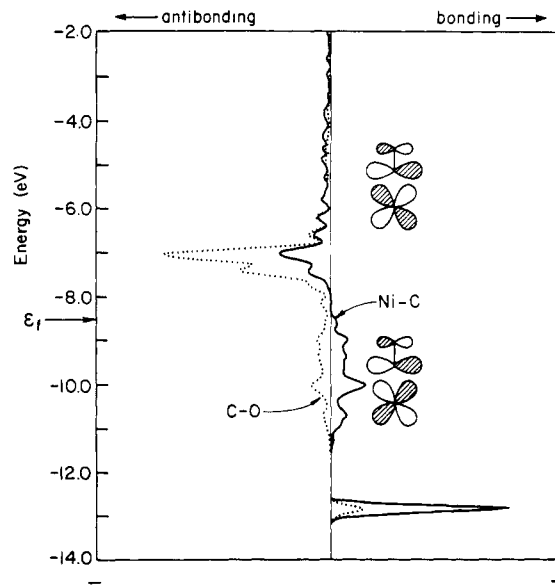**Figure 8.** Crystal orbital overlap population in the c(2×2)CO–Ni(100) chemisorption system.

computed COOP curve for the surface plus adsorbate. Note that the curves, which are sums over all orbitals, nevertheless pick up the features of the 2π and d_π DOS and that signs of the overlap populations follow the above simple picture. Thus the region immediately below ϵ_F is M–C bonding and C–O antibonding, and that above the Fermi level is antibonding M–C and C–O.

Our general point of view, not at all different from that of other workers,[5,17-20] is that 5σ and 2π bind the molecule to the surface. These are the same forward- and back-donating interactions that operate in discrete transition-metal complexes. How is the CO bond then actually broken, following chemisorption or bonding? We do not trust the extended Hückel calculations sufficiently to compute a reaction path. Instead we choose to concentrate on the population of 2π, as others have done.[17,18] Presumably when the bond is sufficiently weakened by population of this CO antibonding orbital, at some point a further sideways motion ensues, with splitting of CO, and coordination of separate C and O to the surface. We will see that as we move from Ni to Fe, Cr, and Ti that population of 2π will rise significantly.

The electron density change of d_δ or $d_{x^2-y^2}$ and d_{xy} orbitals is very small in this system. These orbitals have locally two perpendicular nodal planes which cannot be found in any CO orbitals. Therefore they do not interact with their proximal CO. However, the 2π orbitals may interact with d_δ sets of neighboring metal atoms, as indicated in **7**. Of course, these interactions are weak.

7
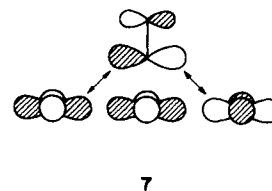
The overlap between one CO 2π and one $d_{x^2-y^2}$ of neighboring metal is 0.011 for Ni, and slightly larger (0.020) for Ti.

It would be nice to have a simple interaction diagram for CO on a surface, just the way we draw them for discrete transition-metal complexes. We do understand all the interactions, as the above discussion shows, but still it is difficult to draw a simple

(16) Hughbanks, T.; Hoffmann, R. *J. Am. Chem. Soc.* **1983**, *105*, 1150.

(17) Anderson, A. B.; Hoffman, R. *J. Chem. Phys.* **1974**, *61*, 4545.
(18) (a) Kobayashi, H.; Yoshiba, S.; Yamaguchi, M. *Surf. Sci.* **1981**, *107*, 321. (b) Kobayashi, H.; Yamaguchi, M.; Yoshida, S.; Yonezawa, T. *J. Mol. Catal.* **1983**, *22*, 205.
(19) Ray, N. K.; Anderson, A. B. *Surf. Sci.* **1982**, *119*. 35.
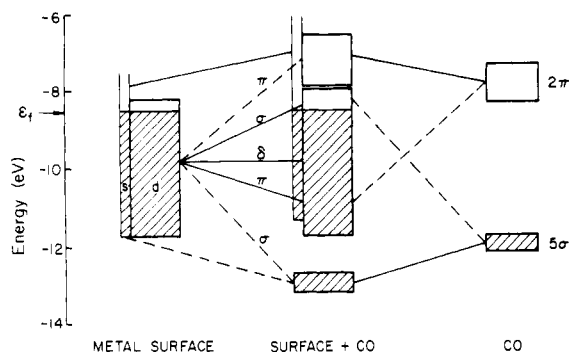(20) Bagus, P. S.; Nelin, C. J.; Bauschlicher, C. W., Jr. *Phys. Rev. B*. **1983**, *28*, 5423.

Figure 9. Principal interactions in the c(2×2)CO–Ni(100) chemisorption system. The solid lines indicate major contributions while dashed lines point to weaker mixing. The open bars are meant to indicate that there is a substantial number of states at still higher energy.
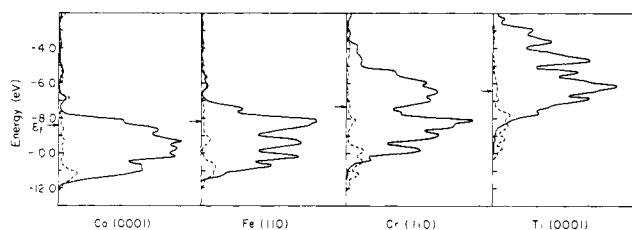

Figure 10. Calculated DOS of the surface layer of Co, Fe, Cr, and Ti four-layer slabs. Solid lines are the projected d states and broken lines the projected s states; the arrow indicates the Fermi level.

diagram, one that is easily portable. Figure 9 is a try at one. The reader is directed to the work of van Santen[5c] for an analysis that bears substantial similarities to ours and also attempts to draw a generalized interaction diagram for CO chemisorption.

Different Transition-Metal Surfaces

To compare the chemisorption behavior of different surfaces we did calculations of CO on Ni(100), Ni(111), Co(0001), Fe-(110), Cr(110), and Ti(0001) surfaces. The first layer of these surfaces is shown in **8**.

8
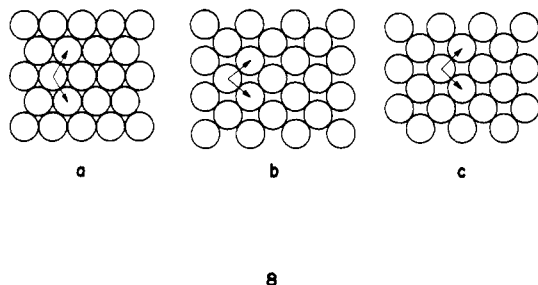
8a is a two-dimensional hexagonal lattice, which represents the first layer of Ni(111), Co(0001), and Ti(0001), because the geometry of the first two layers of fcc(111) and hcp(0001) surfaces is the same. **8b** is a two-dimensional oblique lattice representing the bcc(110) surface for Fe(110) and Cr(110). **8c** is a two-dimensional square lattice representing the Ni(100) surface. The angles between the two lattice vectors in **8a**, **8b**, and **8c** are 120° (or 60°), less than 90°, and 90°, respectively.

In our calculations, a 14K point set[13] was used for the hexagonal lattice of Ni(111), Co(0001), and Ti(0001), a 12K point set[13] for the oblique lattice of Fe(110) and Cr(110), and a 15K point set[13] for the square lattice of the Ni(100) surface. The slab model contains four layers of metal atoms in each case. Figure 10 is the calculated density of states curve of the surface layer of the Co, Fe, Cr, and Ti slabs. The solid lines are the DOS of the d states and the broken lines those of s states. Note first that the d bands go up from Ni to Ti, as do the Fermi levels. Meanwhile the s band energies change very little. This is because the d orbital H_{ii}'s go up while the s H_{ii}'s change much less (see Appendix). Second, from Ni to Ti the d band widths increase. This is because

Table II. Calculated Metal Surface Electronic Structure

	surfaces				
	Ti(0001)	Cr(110)	Fe(110)	Co(0001)	Ni(100)
	Electron Densities on Surface Layer				
s	0.80	0.78	0.71	0.68	0.62
p_σ	0.06	0.07	0.07	0.06	0.04
p_π	0.14	0.28	0.21	0.20	0.15
d_σ	0.50	1.06	1.61	1.81	1.93
d_π	1.20	2.05	3.14	3.57	3.81
d_δ	1.21	2.12	2.81	3.20	3.63
total	3.91	6.35	8.55	9.52	10.17
	Fermi Levels				
ϵ_f, eV	−6.47	−7.35	−8.17	−8.42	−8.59

the d orbitals are becoming more and more diffuse. The computed electronic distribution of these surfaces is presented in Table II.

What are the differences when carbon monoxide adsorbed on these surfaces? As in the c(2×2)CO–Ni(100) system, we use a four-layer metal slab with CO adsorbed on one side, on top. Bridging adsorption will be discussed later.

In order to save computing time a smaller unit cell containing four metal atoms and one carbon monoxide molecule is used in the calculations. This corresponds to full coverage, $\theta = 1$, while in the c(2×2)CO–Ni(100) system we worked with $\theta = 0.5$. It is obvious that in the smaller unit cell the CO–CO interaction is overemphasized. The CO band widths are exaggerated. The calculational results are listed in Table III. A comparison of the electron densities and overlap populations of the small cell Ni-(100)–CO system in Table III with those for c(2×2)CO–Ni(100) in Table I shows that the difference is very small, comparing with the difference between different metals. This tells us the small unit cell simplification is adequate, and it also informs us that coverage has much less effect on surface–adsorbate interactions than the electronic nature of the surface.

Let us analyze the trends as one moves from a Ni to a Ti surface interacting with carbon monoxide. The d bands move up in energy along that series, as Figure 10 showed. Thus, the interaction between d_σ and 5σ of CO should decrease, because 5σ is below the metal d bands. Also the d electron count decreases, therefore Δd_σ gets smaller in absolute value. Meanwhile, the s bands change very little in energy and the s electron number is even larger (see Table II), therefore Δs increases in absolute value. However, the Δd_π remains almost unchanged at about −0.3. Unlike d_{z^2} and s orbitals, which interact mainly with CO 5σ orbitals, d_π or $d_{xz,yz}$ orbitals interact mainly with CO 2π orbitals. 5σ orbitals are lower in energy than metal orbitals, but 2π orbitals are higher and close to the metal orbitals, especially to the d bands. As the metal d bands go up from Ni to Ti, their interaction with 5σ gets smaller, but their interaction with 2π increases. Another factor is the band width of the d states, which increases from Ni to Ti, and thus allows mixing with 2π orbitals over a wide range. Furthermore, the Fermi level is rising from Ni to Ti,[21] making electron transfer to 2π of CO easier. All of these factors reinforce in a natural way.

It should be noted that this discussion of the special role of CO 2π and its energy relative to the metal band is not original to us. It has been made by others, particularly in the work of Anderson.[22]

Let us look at the extreme case, the Ti(0001) surface, in some detail. Figure 11 shows the part of the DOS that is on CO 2π on that surface. The lower part of the d band contains most of the 2π density. In contrast in Ni(100) we saw that the major part of the DOS of 2π is above the Fermi level.

(21) It should be noted that our calculations do not reproduce well the absolute value of the metal work functions. These are 4.3 eV (Ti), 4.5 eV (Cr), 4.5 eV (Fe), 5.0 eV (Co), 5.2 eV (Ni) for polycrystalline films: Eastman, D. E. *Phys. Rev.* **1970**, *82*, 1.

(22) Ray, N. K.; Anderson, A. B. *J. Phys. Chem.* **1982**, *86*, 4851; *Surf. Sci.* **1983**, *125*, 803. See also: Russell, J. W.; Overend, J.; Scanlon, K.; Severson, M.; Bewik, A. *J. Phys. Chem.* **1982**, *86*, 3066. Russell, J. W.; Severson, M.; Scanlon, K.; Overend, J.; Bewik, A. *J. Phys. Chem.* **1983**, *87*, 293. Brodén, G.; Gafner, G.; Bonzel, H. P. *Surf. Sci.* **1979**, *84*, 295.

Table III. Some Computational Results of CO Chemisorption Systems

	Ti(0001)	Cr(110)	Fe(110)	Co(0001)	Ni(100)	Ni(111)
			substrates			
			Overlap Populations			
M–C	1.11	0.93	0.91	0.83	0.78	0.75
C–O	0.43	0.87	0.96	1.01	1.03	1.02
			CO Electron Densities			
5σ	1.73	1.67	1.62	1.60	1.60	1.59
2π	1.61	0.74	0.54	0.43	0.39	0.40
			Electron Density Changes on the Surface Layer[a]			
Δs	−0.18	−0.18	−0.14	−0.13	−0.07	−0.08
Δp_σ	0.15	0.17	0.15	0.15	0.15	0.14
Δp_π	0.03	−0.05	0.01	0.00	0.03	0.01
Δd_σ	−0.01	−0.16	−0.57	−0.66	−0.53	−0.65
Δd_π	−0.31	−0.39	−0.31	−0.33	−0.43	−0.36
Δd_δ	−0.26	−0.23	−0.07	−0.09	−0.00	−0.03
total	−0.57	−0.84	−0.92	−1.06	−0.85	−0.96
			Other Layers			
total	−2.29	−0.17	0.37	0.75	0.60	0.72
ΔE,[b] eV	−6.77	−3.44	−2.64	−1.98	−1.97	−1.66

[a] Electron density changes of the surface layer on which the CO's are adsorbed. These numbers are the differences from those of Table II. [b] E(adsorption system) − ($E_{\text{clean slab}} + E_{CO}$) per unit cell (four metal atoms and one CO).
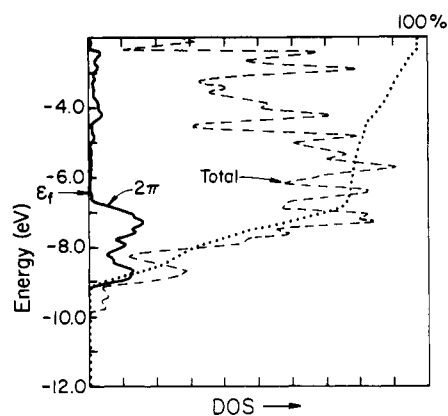

Figure 11. Projected DOS of 2π of CO on the Ti(0001) surface. The dotted line is the integrated DOS of 2π. The broken line is the total DOS of the chemisorption system.

In summary, the population of carbon monoxide 2π increases steadily from Ni to Ti. The CO bond is much weakened, its overlap population down to 0.43 on Ti(0001) from 1.02 on Ni(100) and 1.21 in free CO. We would anticipate a greater ease of CO cleavage as one moves to the left in the transition series, and indeed this is what is observed.

Different Surfaces of the Same Metal

Table III allows a comparison of the adsorption of CO on Ni(111) vs. Ni(100). We find that the (111) surface weakens the C–O bond a little more than the (100) surface. This is in agreement with some experimental[23,24] and theoretical[18b] studies. However, the matter is complicated because different adsorption sites are involved in the experimentally observed species. One of the reviewers of this paper pointed out that the trend in C–O bond weakening might have been expected to be (100) > (111), since the work function of low-index surfaces is smaller than that of high-index ones.[25] Also in the case of a stepped surface, the extreme case of a low-index surface, there are indications of substantial CO weakening.[26] We are not certain here of the

overall strength of either the experimental conclusions or our theoretical results. What is clear is that the difference between different surfaces of a given metal is less than that arising from changing the metal.

Different Adsorption Sites

For CO adsorption on Ni(111) it is reported that CO is bound mainly in a bridging position,[24a,c] while for CO on Ni(100) it is known that the relative proportion of bridge-bonded and on-top CO is strongly dependent on adsorption temperature and coverage.[24b] The extended-Hückel method is not very good at determining bond distances, and the comparison by this method of two isomers which differ substantially in geometry is problematic. Nevertheless, we think the topology of the interactions and their magnitude is correctly given by this approximate procedure. Thus we proceeded to carry out calculations for twofold bridge and threefold bridge site adsorption on Ni(111), **9** and **10**.

Two-fold bridge   Three-fold bridge
9   **10**

○ CO
◯ Ni
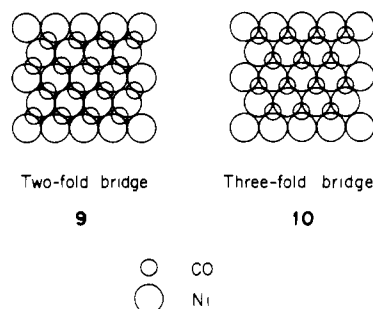
The computational results are shown in Table IV, which include the on-top adsorption result for comparison. In each bridge site we did two calculations, one at a Ni–C distance of 1.80 Å the other at a perpendicular carbon–surface layer distance of 1.80 Å. Compared to on-top adsorption, the metal surface d_{z^2} electron density changes are much smaller, while those of the $d_{xz,yz}$ set are larger. This is because on bridge-site adsorption the metal d_{z^2} orbitals are no longer pointed directly at CO. Instead d_{xz}, d_{yz} orbitals are now oriented for interaction. Meanwhile $\Delta d_{x^2-y^2}$, Δd_{xy} become larger in absolute value because of larger overlap with CO orbitals.

In the C–surface perpendicular distance 1.80-Å case, it has almost the same 2π electron density and the C–O overlap population as in the case of on-top adsorption. Unfortunately, the result

(23) Iwasawa, Y.; Mason, R.; Texter, M.; Somorjai, G. A. *Chem. Phys. Lett.* **1976**, *44*, 468.

(24) (a) Brodén, G.; Pirug, G.; Bonzel, H. P. *Chem. Phys. Lett.* **1977**, *51*, 250. (b) Andersson, S. *Solid State Commun.* **1977**, *21*, 75. (c) Bertolini, J. C.; Dalmai-Imelik, G.; Rousseau, J. *Surf. Sci.* **1977**, *68*, 539. (b) Compuzano, J. C.; Greenler, R. G. *Surf. Sci.* **1979**, *83*, 301.

(25) Hölzl, J. In "Solid Surface Physics", Springer-Verlag: Berlin, 1979; p 75.

(26) Erley, W.; Ibach, H.; Lehwald, S.; Wagner, H. *Surf. Sci.* **1979**, *83*, 585.

584 *J. Am. Chem. Soc., Vol. 107, No. 3, 1985*

Sung and Hoffmann

Table IV. Comparison of Different Adsorption Sites on the Ni(111) Surface

geometry	on top	bridge adsorption			
		$d_\perp = 1.80$ Å[c]		$d_{Ni-C} = 1.80$ Å[d]	
		2-fold	3-fold	2-fold	3-fold
Overlap Populations					
Ni–C	0.76	0.31	0.16	0.57	0.41
C–O	1.02	1.02	1.02	0.97	0.93
CO Electron Density					
5σ	1.59	1.57	1.54	1.57	1.56
2π	0.40	0.41	0.41	0.54	0.64
Electron Density Changes in the Surface Layer[a]					
Δs	−0.08	−0.14	−0.14	−0.15	−0.16
Δp_z	0.14	0.11	0.07	0.12	0.07
$\Delta p_{x,y}$	0.01	0.01	0.04	0.02	0.08
Δd_{z^2}	−0.65	−0.39	−0.33	−0.29	−0.28
$\Delta d_{xz,yz}$	−0.36	−0.33	−0.44	−0.66	−0.66
$\Delta d_{xy,x^2-y^2}$	−0.03	−0.13	−0.11	−0.43	−0.47
total	−0.96	−0.87	−0.89	−1.39	−1.43
Other Layers					
total	0.72	0.61	0.64	0.94	0.78
ΔE,[b] eV	−1.66	−0.89	−0.71	−2.72	−3.24

[a,b] As in Table III. [c] The distance between the carbon atom and the metal surface is 1.80 Å. In these geometries $d_{Ni-C} = 2.19$ and 2.3 Å for the 2-fold and 3-fold bridge case, respectively. [d] The distance between the carbon atom and the nearest metal atom is 1.80 Å. In these geometries $d_\perp = 1.30$ and 1.08 Å for the 2-fold and 3-fold bridge case, respectively.

Table V. Extended Hückel Parameters

orbital	H_{ii}, eV	ζ_1	ζ_2	C_1[a]	C_2[a]
Ti 4s	−6.3	1.50			
Ti 4p	−3.2	1.50			
Ti 3d	−5.9	4.55	1.40	0.4206	0.7839
Cr 4s	−7.3	1.70			
Cr 4p	−3.6	1.70			
Cr 3d	−7.9	4.95	1.60	0.4876	0.7205
Fe 4s	−7.6	1.90			
Fe 4p	−3.8	1.90			
Fe 3d	−9.2	5.35	1.80	0.5366	0.6678
Co 4s	−7.8	2.00			
Co 4p	−3.8	2.00			
Co 3d	−9.7	5.55	1.90	0.5550	0.6460
Ni 4s	−7.8	2.1			
Ni 4p	−3.7	2.1			
Ni 3d	−9.9	5.75	2.00	0.5683	0.6292
C 2s	−18.2	1.63			
C 2p	−9.5	1.63			
O 2s	−29.6	2.27			
O 2p	−13.6	2.27			

[a] Contraction coefficients used in the double-ζ expansion.

depends on the C–surface distance. At C–Ni = 1.80 Å the bridge site properties are quite different from those of the on-top site. For one distance the bridge adsorption energy is smaller and for the other distance larger than for on-top binding. This is discouraging, for we cannot decide if bridge bonding is favored. In nickel carbonyl complexes the Ni–C distances are very similar

for terminal and bridged carbonyls.[27] Our feeling is that the bridge-adsorbed CO should have a Ni–C distance between the two cases listed in Table IV. Consequently, the bridge-adsorbed carbonyls should have a higher 2π occupation and a weaker CO bond.

Conclusion

When CO molecules are adsorbed in on-top sites on transition-metal surfaces, the CO 5σ orbitals interact with metal d_{z^2} and s states and CO 2π orbitals interact with metal $d_{xz,yz}$. These are the same interactions that occur in discrete transition-metal carbonyls. There is little mixing of these two types of orbitals, and indeed CO low-lying orbitals and metal p orbitals do not get much involved. The metal–CO 2π back-bonding determines the dissociative behavior of the carbonyl. From Ni to Ti the Fermi level rises, the d orbitals become more diffuse, and as a consequence the CO 2π levels gain more and more electron density. This is why CO dissociates on the early transition metals.

The coverage of CO has little effect on CO dissociation. In our calculations the higher index surface would seem to have a tendency to dissociate CO more easily than the lower index one. However, this is a secondary effect compared to the electronic nature of the metal itself.

Appendix

All the calculations were of the tight-binding extended-Hückel type. The H_{ii}'s for transition metals were obtained from earlier work.[12] They were determined by charge iteration on bulk metals, assuming the charge dependence of metal H_{ii}'s given by Gray's equations.[28] The A, B, and C iteration parameters were taken from ref 29. Experimental hcp, fcc, and bcc structures were used. The H_{ii}'s of C and O were determined by charge iteration on CO adsorbed on an Fe(110) slab of four layers, iterated three cycles. The iteration parameters were taken from ref 29 also. Extended-Hückel parameters for all atoms used are listed in Table V.

The geometrical parameters for chemisorption systems are the following: C–O distance 1.15 Å; C–metal atom distances for Ni, Co, Fe, Cr, and Ti are 1.80, 1.82, 1.84, 1.92, and 2.03 Å, respectively.

(27) Ruff, J. K.; White, R. P., Jr.; Dahl, L. F. *J. Am. Chem. Soc.* **1971**, *93*, 2159. Longoni, G.; Chini, P.; Lower, L. D.; Dahl, L. F. *J. Am. Chem. Soc.* **1975**, *97*, 5034.

(28) Ballhausen, C. J.; Gray, H. B. "Molecular Orbital Theory"; W. A. Benjamin, Inc.: New Yrok 1965; p 125.

(29) McGlynn, S. P.; Van Quickenborne, L. G.; Kinoshita, M.; Caroll, D. G. "Introduction to Applied Quantum Chemistry"; Holt, Rinehart and Winston, Inc.: New York, 1972.